

Electron-impact fragmentation of Cl_2^-

G. F. Collins,¹ D. J. Pegg,² K. Fritioff,³ J. Sandström,³ D. Hanstorp,³ R. D. Thomas,⁴ F. Hellberg,⁴ A. Ehlerding,⁴ M. Larsson,⁴ F. Österdahl,⁵ A. Källberg,⁶ and H. Danared⁶

¹*Department of Physics, Queen's University Belfast, Belfast BT7 1NN, Northern Ireland, United Kingdom*

²*Department of Physics, University of Tennessee, Knoxville, Tennessee 37996, USA*

³*Department of Physics, Chalmers University of Technology/Göteborg University, SE-412 96 Göteborg, Sweden*

⁴*Department of Physics, AlbaNova, Stockholm University, 106 91, Stockholm, Sweden*

⁵*Department of Physics, Royal Institute of Technology, AlbaNova, 106 91, Stockholm, Sweden*

⁶*Manne Siegbahn Laboratory, Frescativägen 24, SE-104 05 Stockholm, Sweden*

(Received 2 May 2005; published 14 October 2005)

A merged beam technique has been used to investigate the fragmentation of the Cl_2^- ion in collisions with electrons over an energy range of 0–200 eV. We have measured absolute cross sections for detachment, detachment plus dissociation and dissociation processes. Over the energy range studied, the dominant breakup mechanism is dissociation. Dissociation is relatively enhanced in the $e^- + \text{Cl}_2^-$ collision system due to the suppression of the normally dominant detachment process, as a result of the large difference between the equilibrium internuclear distances of the Cl_2 and Cl_2^- ground state potential curves. A prominent structure is observed just above the threshold in the $\text{Cl}^- + \text{Cl} + e^-$ dissociation channel. It is proposed that the structure is a resonance associated with production and rapid decay of an excited state of the doubly charged Cl_2^- ion. A plausible mechanism for production of the di-anionic state based on an excitation plus capture process is suggested.

DOI: [10.1103/PhysRevA.72.042708](https://doi.org/10.1103/PhysRevA.72.042708)

PACS number(s): 34.80.Kw

INTRODUCTION

Measurements of cross sections for processes involving collisions between electrons and atomic and molecular negative ions are of fundamental interest and also provide important data for the modelling of low temperature plasmas. Experimental studies of such collisions began about forty years ago when Tisone and Branscomb [1] used perpendicularly crossed beams of electrons and H^- ions to measure the cross section for single electron detachment. This work was followed by further crossed beam measurements on H^- and other, more complex, ions [2–5]. The relatively recent advent of heavy ion storage rings dedicated to atomic and molecular physics has allowed such studies to be carried out using merged beams of essentially monoenergetic electrons and negative ions. This technique makes it possible to easily access the threshold region of the cross section with high-energy resolution. The principal reactions induced by electron impact on a negative ion are detachment of one or more electrons from the ion and, in the case of molecular ions, dissociation or detachment plus dissociation. Cross sections for these processes have been studied for a variety of atomic and molecular negative ions, for example, at the ASTRID facility in Aarhus [6–9] and the CRYRING facility in Stockholm [10–12].

Theoretical studies of the dynamics of collisions between electrons and negative ions are complicated by the existence of a long-range Coulomb interaction in the initial state which, when combined with the short-range attractive polarization interaction, results in a repulsive potential barrier. There is considerable interest in the threshold behavior of the cross section for such a collision system. Another phenomenon of current interest is the formation of doubly charged

negative ions or dianions, that can arise if the incident electron is temporarily captured by the negative ion. The lifetime of such a resonance is essentially determined by the ability of the system to accommodate the additional Coulomb energy arising from the electron capture. The localization of electrons in smaller systems such as atomic negative ions prohibits the formation of dianions [13]. Larger systems are, however, sometimes capable of temporarily binding two extra electrons [14–17]. Stable dianions such as Cl_2^{2-} [18] can be formed once the molecule is sufficiently large to accommodate two additional electrons.

The destruction of atomic and molecular negative ions by electron impact plays an important role in many physical processes in both astrophysical and laboratory plasmas. One important application of halogen ions is in the plasma etching industry. Molecular chlorine, Cl_2 , is used as a plasma processing gas in the etching of semiconductors. The active components of the plasma used to etch the silicon surface are atomic Cl and the atomic ions, Cl^+ and Cl^- . These components are formed in dissociation and dissociative attachment processes when electrons collide with Cl_2 molecules. In addition, the molecular ions, Cl_2^+ and Cl_2^- , are produced by electron impact ionization and attachment, respectively. The efficiency of the etching process is somewhat unreliable since instabilities in the plasma are caused by changes in the electron-ion equilibrium. Christophorou and Olthoff [19] have made an extensive study of electron-induced interactions in the case of Cl_2 , however modelling of these plasmas has so far neglected the role played by Cl_2^- as no information has been available to date on electron impact collisions involving this negative ion.

In the present experiment we have used a merged beam apparatus to measure absolute cross sections for the pro-

cesses of pure detachment, detachment plus dissociation and pure dissociation following a collision between an electron and the Cl_2^- molecular ion in the energy range 0–200 eV. Calculations of such processes for the Cl_2^- ion are currently unavailable but a recent experimental study of the homologue ion F_2^- by Pedersen *et al.* [21] has provided us with the opportunity to investigate the similarities and differences between the two collision systems. Pedersen *et al.* measured cross sections for the fragmentation of the F_2^- molecular ion following electron impact over the energy range 0–27 eV. Three reactions with the following final states were studied: $\text{F}_2 + 2e^-$ (detachment), $\text{F} + \text{F} + 2e^-$ (detachment plus dissociation), and $\text{F} + \text{F}^- + e^-$ (dissociation). One interesting observation from this work was that dissociation dominated the breakup of F_2^- . The cross section for dissociation was an order of magnitude larger than the total detachment cross section and two orders of magnitude larger than the dissociation cross sections of other negative ions. In essentially all other experiments involving electron collisions with atomic and molecular negative ions, the ion is primarily destroyed by pure detachment leaving a neutral atom or molecule. It was shown that the potential energy curves for F_2^- were significantly different from those of other homonuclear molecular negative ions that had been investigated previously by the same research group [9]. The unusual behavior of cross sections in the case of the $e^- + \text{F}_2^-$ system can be traced to the relatively large difference of 0.5 Å between the equilibrium internuclear distances of F_2^- and F_2 . This situation leads to an unfavorable overlap of the nuclear wave functions in the anionic and neutral systems and hinders autodetachment via low-lying repulsive curves of F_2^- . We have found that a similar situation exists in the case of the $e^- + \text{Cl}_2^-$ system. Figure 1 shows the relative positions of the lowest-lying potential energy curves based on the calculations of Leininger and Gadea [22]. In the figure we show the ground state potential curves for Cl_2^- and Cl_2 and three low-lying repulsive curves of Cl_2^- . The calculation also predicts that the difference between the equilibrium internuclear distances in this case is close to 0.6 Å. As a result of this rather large separation, the process of detachment is suppressed, as it was for the $e^- + \text{F}_2^-$ system. At low energies, it is clear from Fig. 1 that the Cl_2^- ion will preferentially dissociate via the low-lying repulsive curves of Cl_2^- , thus we saw similarities between the $e^- + \text{Cl}_2^-$ and $e^- + \text{F}_2^-$ collision systems, as might be expected. The most interesting outcome of the present study, however, was the observation of a major difference between the two collision systems. In this work we observed a broad, and relatively intense, structure in the cross section for the $\text{Cl}^- + \text{Cl} + e^-$ dissociation channel that is absent in the corresponding channel for the $e^- + \text{F}_2^-$ system. It is suspected that the structure arises from the production and decay of a short-lived resonance associated with the temporary formation of a doubly charged Cl_2^{2-} ion. Possible reasons for the presence of the resonance in the $e^- + \text{Cl}_2^-$ system but its absence in the $e^- + \text{F}_2^-$ system will be discussed later in the paper.

EXPERIMENTAL PROCEDURES

The merged electron-ion beam experiment was performed at the CRYRING storage ring facility at the Manne Siegbahn

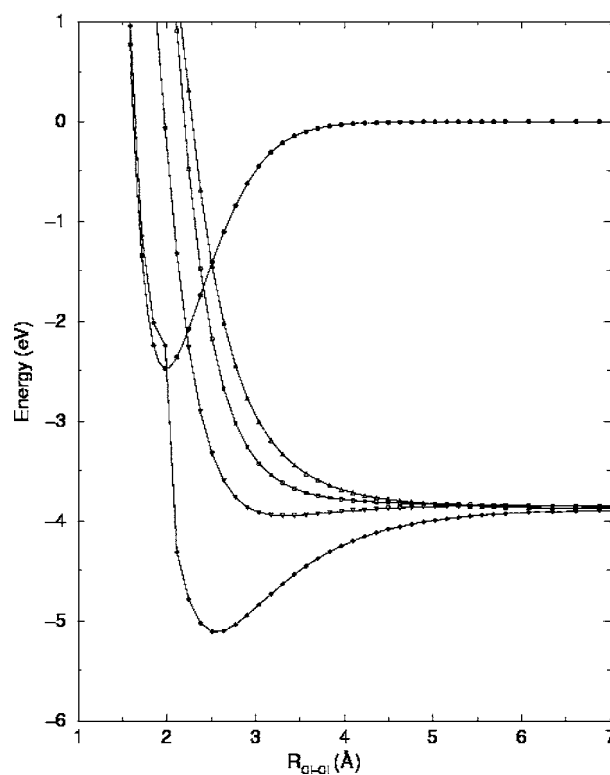


FIG. 1. An energy diagram showing the relative positions of the lowest potential energy curves as calculated by Leininger and Gadea [22]. The upper line represents the ground state of the Cl_2 molecule. The lower four curves represent the ground state of Cl_2^- and three unbound excited states.

Laboratory in Stockholm. The general apparatus and experimental technique has been described in detail in a previous publication [11]. The Cl_2^- ions were produced in a sputter ion source and injected into the ring, where they were accelerated to 1.3 MeV. Over time, the ions that circulate in the ring are destroyed in collisions with the residual gas particles. The stored lifetime of the ions in the ring, which is determined by the ring pressure and the energy of the ions, was approximately one second in the present experiment. Each ring cycle consisted of five phases: injection, acceleration, cooling, measurement and the dumping of the beam to terminate the cycle. The data is accumulated over many ring cycles. During each cycle the ion beam was merged with an electron beam over a distance of 85 cm. This section of the ring is called the cooler. In the cooling phase, the velocity spread of the ions in the beam was reduced by phase space cooling during their interaction with velocity-matched electrons. In the measurement phase of the cycle the velocity of the electrons is increased or decreased relative to the fixed velocity of the ions in order to create finite collision energies in the center-of-mass frame. The velocity of the electrons is changed by ramping the acceleration voltage on the electron gun in the cooler. In the present case, collision energies in the range 0–200 eV were used. The detectors of the collision products were situated downstream of the cooler, which becomes the interaction region for the electron-ion collision experiments. Figure 2 shows the positioning of the detectors relative to the interaction region. The heavy particle frag-

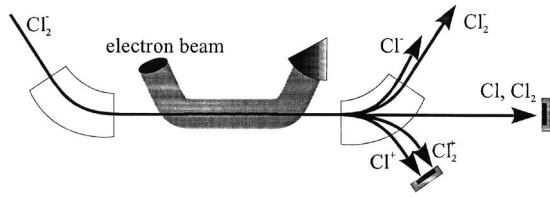
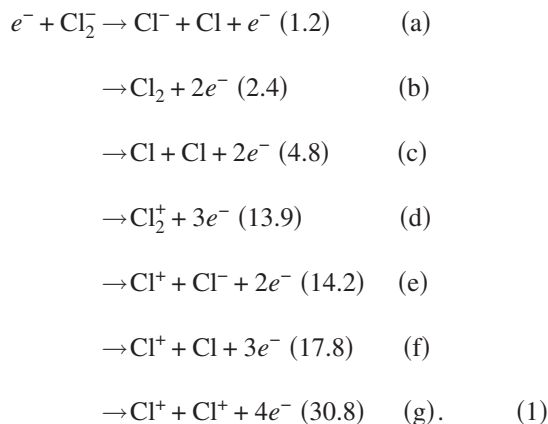


FIG. 2. A schematic of the electron-negative ion interaction region and the downstream detectors used to monitor neutral and single positively charged ion fragments produced in the interaction region.

ments produced in the collision were charge-state analyzed prior to detection. The output of two detectors constituted the signals in the experiment. One detector collected neutral particles (Cl_2 and Cl) and the other detector collected singly charged positive ions (Cl_2^+ and Cl^+). It was not possible to detect negatively charged products in this experiment since their trajectories were bent in the same direction as the primary negatively charged ion beam. The detectors are energy-sensitive surface barrier detectors. The output of such a detector consists, in general, of a series of peaks representing particles of different masses but with the same charge state. Thus, in the present experiment, the output of both the neutral particles detector and the positive ion detector consisted of two peaks corresponding to product particles of mass 35 (Cl or Cl^+) and mass 70 (Cl_2 , $\text{Cl}+\text{Cl}$ or Cl_2^+ , Cl^++Cl^+).

The following channels were energetically accessible in the energy range of the present experiment. The threshold energies are shown, in eV, in parentheses. The energies were determined by using the known dissociation energy of Cl_2^- (1.2 eV), the adiabatic electron affinity of Cl_2 (2.4 eV), the ionization energy of Cl_2^+ (11.5 eV), the electron affinity of Cl (3.6 eV) and the ionization energy of Cl^+ (13 eV):



Reactions (a) and (f) contribute to the mass 35 peak in the neutral particle detector. Reactions (b) and (c) will contribute to the mass 70 peak in the neutral particle detector. Reactions (e) and (f) will contribute to the mass 35 peak in the positive ion detector and reactions (d) and (g) will contribute to the mass 70 peak in the same detector. The reaction (g), which would have contributed to the mass 70 peak in the positive ion detector, was not observed in the experiment presumably because it was weak at the energies studied. The reactions (a) and (f) can be separated because reaction (f) can also be

detected using the positive ion detector. It is not possible, however, to distinguish between reactions (b) and (c) because the products of both reactions will contribute to the mass 70 peak in the neutral particle detector only. To overcome this problem we have used the so-called grid technique to separate these channels [23]. When a grid of known transmission, T , is placed in front of the detectors, each product particle will be transmitted with identical probability, T . In effect there will be a redistribution of the counts in each mass peak arising from the insertion of the grid enables one to determine branching ratios for the different reactions and separate reactions such as (b) and (c).

The cross section for fragmentation of a negative ion following electron impact is proportional to the rate of production, R , of the final state heavy particle fragments that is used as the signature of the selected reaction. If we assume that the particles in the electron and ion beams are uniformly distributed, an operational expression for the cross section can be written in the form

$$\sigma = Rv_i e^2 / (v_r n_e I_i L), \quad (2)$$

where R is the reaction rate, as measured by the number of signal counts per second. The symbols v_i and v_r represent the ion velocity and the relative velocity of the ions and electrons, respectively and L is the length of the interaction region. The quantity $n_e = I_e / Av_e$ represents the density of a beam of electrons of cross sectional area, A , that have a velocity, v_e , and a current I_e . The ion beam current, I_i , is proportional to the rate of destruction of the ions due to collisions with particles of the residual gas in the ring.

Absolute measurements of cross sections are relatively straightforward when a storage ring is used. The geometry of the overlap of the two beams is well known since the cooled ion beam is usually much smaller than the electron beam. The distribution of electrons is approximately constant in the overlap region. In addition, the efficiencies for collection and detection are essentially unity at the incident particles energies used in the experiment. Two corrections however must be made to the measured cross section. Electrons in the beam experience a space charge effect that changes their energies slightly. The correction can easily be calculated knowing the intensity and geometry of the electron beam. Secondly, toroidal deflectors are used in the cooler to bend the electron beam in and out of the interaction region. Events originating in the merging and demerging regions also contribute to the signal. The collision energies in this case will, however, be larger than that arising from the region where the ion and electron beams are collinearly merged. A correction can be applied to the measured cross section since the geometry of the merge and demerge regions is well known.

We estimate the overall uncertainty in the absolute cross sections to be about 20%. Statistical uncertainties are associated with the signals from the surface barrier detectors and in the measurement of the ion beam current. These uncertainties are typically less than 10%. The dominant contribution to the total systematic uncertainty arises from the measurement of the ion beam current (5–15%) and the length of the interaction region (5%). In addition, there are uncertainties

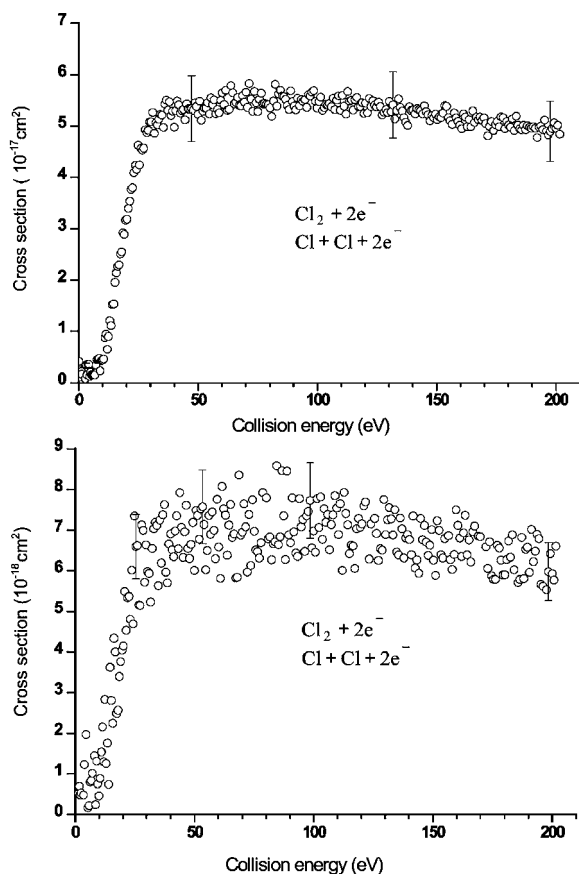
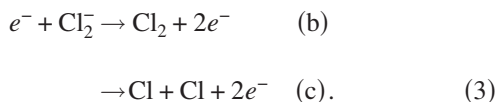


FIG. 3. The upper part of the figure shows the total cross section associated with the detection of mass 70 fragments ($\text{Cl}_2, \text{Cl}+\text{Cl}$) in the neutral detector. The lower part of the figure shows how the cross section changes when a grid is placed in front of the detector. The reaction channels that contribute are also shown.

associated with the measurement of the electron beam current (2%), the diameter of the electron beam (1%), the circumference of the storage ring (0.5%) and the orbital frequency of the ions (>0.01%). The toroidal correction contributes with an uncertainty of 2%.

RESULTS

The measured cross section for the production of neutral mass 70 fragments ($\text{Cl}_2, \text{Cl}+\text{Cl}$) is shown in Fig. 3. The upper part of the figure shows the total cross section for the sum of two reactions. It contains contributions from detachment and detachment plus dissociation channels:



The lower part of the figure shows the output of the same detector with a grid placed in front of it. A fraction of the atoms produced by reaction (c) will be stopped by the grid. If only one of the atoms is stopped, these events will end up in the mass 35 peak. We are able to calculate this redistribution of counts since the transmission of the grid is known to be

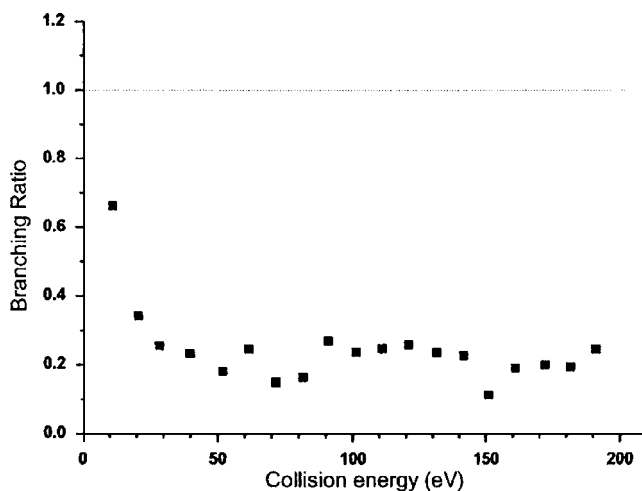
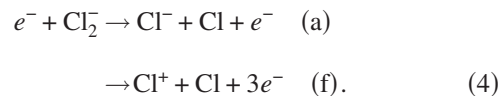


FIG. 4. Ratio of detachment leading to a molecular fragment in the final state, $\text{Cl}_2 + 2e^-$, relative to the detachment plus dissociation cross section.

0.296(15) [20]. The grid technique was used to determine the branching ratios for the two reactions shown in Eq. (3). The fraction of ions that are destroyed by the detachment process is shown in Fig. 4. The figure shows that the cross section without the grid is primarily associated with the $\text{Cl}+\text{Cl}+2e^-$ channel. The ratio is highest at low electron energies but drops to an approximately constant value of 0.2 above 30 eV. As stated previously, the dominance of dissociation over detachment is unusual but was observed in the corresponding reactions involving the F_2^- ion. This is a result of the fact that the equilibrium internuclear distances of the molecules and the molecular negative ions differ much more in the case of the halogens than for most other elements. The shape and magnitude of the cross section shown in Fig. 3 is similar to that of the corresponding cross section for other negative ions. It increases relatively sharply from threshold to a maximum of $5.7 \times 10^{-17} \text{ cm}^2$ at 70 eV. The cross section then smoothly decreases up to the highest energy used in the experiment, 200 eV. However, the electron affinity of Cl_2 is 2.45 eV and the threshold for detachment is about a factor of four larger than this. This difference associated with the Coulomb repulsion in the initial state of the reaction, is similar to that observed in the case of detachment from the F_2^- [21]. The minimum energy of 5 eV (the electron affinity plus the dissociation energy of the Cl_2 molecule) required for detachment plus dissociation is also smaller than the observed threshold. A similar situation was reported by Pedersen *et al.* [21] in the case of F_2^- .

The measured cross section for the production of neutral mass 35 fragments (Cl) in $e^- + \text{Cl}_2^-$ collisions is shown in Fig. 5. The upper part of the figure shows the signal from the neutral particle detector. This cross section contains contributions from the dissociation and detachment plus dissociation channels



The lower part of the figure shows the output of the same detector with a grid placed in front of it. The insertion of a

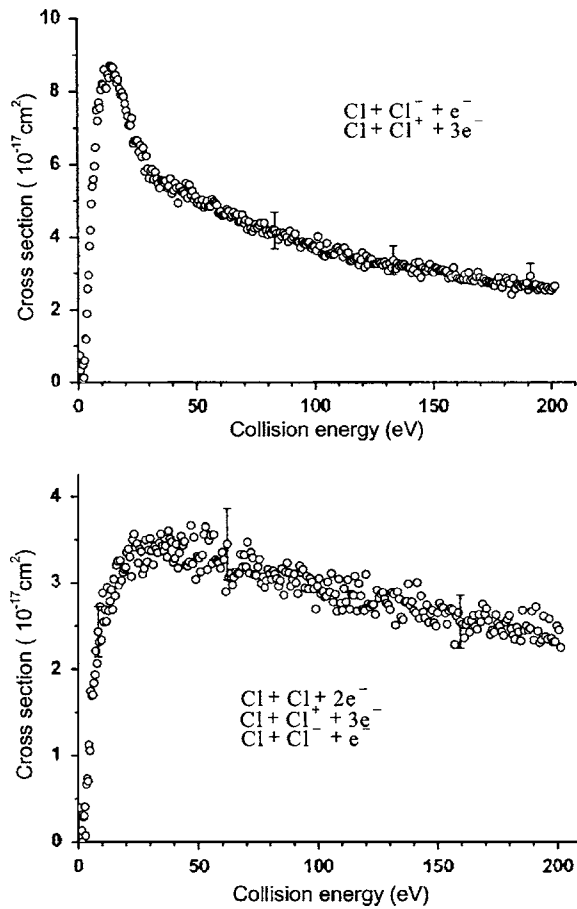


FIG. 5. The upper part of the figure shows the total cross section associated with the detection of mass 35 fragments (Cl) in the neutral detector. The lower part of the figure shows how this signal changes when a grid is placed in front of the detector. The reaction channels that contribute are also shown.

grid causes a redistribution of the counts in the two mass peaks of the neutral particle detector. In this case, some counts from the mass 70 peak are transferred to the mass 35 peak. The cross section was reduced by only 25% when the grid was inserted. This observation provides further evidence that a large contribution to the cross section shown in the upper part of Fig. 3 is associated with the $\text{Cl} + \text{Cl} + 2e^-$ channel. The most significant feature of the total cross section shown in Fig. 5 is the structure that appears just above threshold. The lower part of the figure shows that this structure is no longer apparent when a grid is placed in front of the neutral detector. The addition of a strong signal from the $\text{Cl} + \text{Cl} + 2e^-$ channel when the grid is inserted is sufficient to wash out the structure. It is thought that the structure is a resonance in the $\text{Cl} + \text{Cl}^- + e^-$ channel. This will be discussed further in a later section.

The measured cross sections for the production of positively charged particles of mass 35 and 70 are shown in Figs. 6 and 7, respectively. The following reaction channels contribute to the signal associated with the mass 35 peak (Cl^+) in the output of the positive ion detector

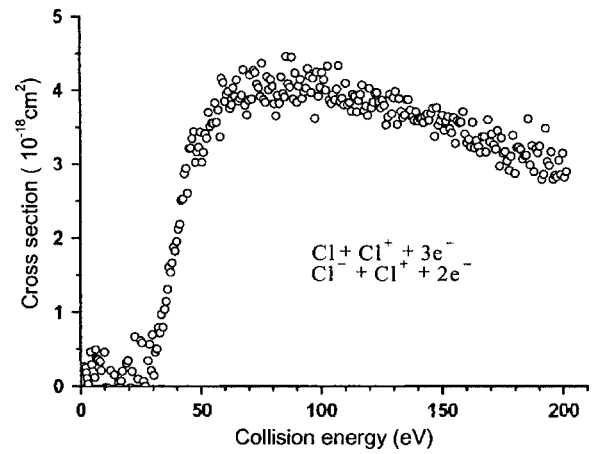
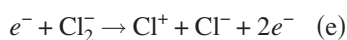
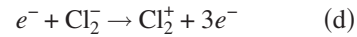


FIG. 6. Total cross section associated with the detection of mass 35 fragments (Cl^+) in the positive ion detector. The reaction channels that contribute to the cross section are also shown.



The cross section rises from threshold to a peak value of about $4.2 \times 10^{-18} \text{ cm}^2$ around 70 eV. The measured threshold is about 30 eV. The following reaction channels could contribute to the signal associated with the mass 70 peak (Cl_2^+ , $\text{Cl}^+ + \text{Cl}^+$) in the positive ion detector



The reaction channel (g) apparently has a small cross section and a signal from the reaction was not observed in the present experiment. The reaction channels (d) and (g) are distinguishable even though they both involve detecting ions whose combined mass was 70. This is possible since Cl_2^+ and Cl^+ have different trajectories in the magnetic field and are therefore spatially separated at the detector (see Fig. 2).

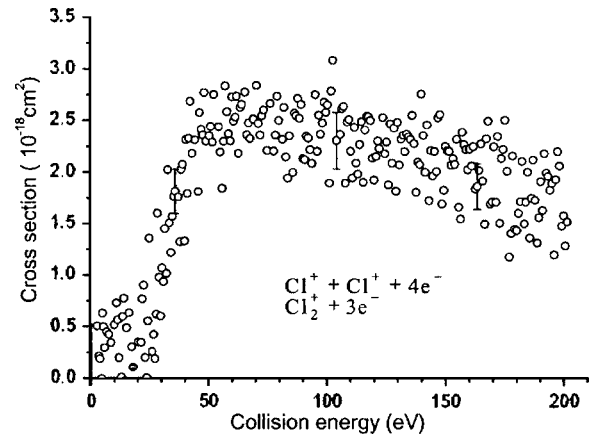
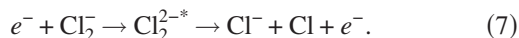


FIG. 7. Total cross section associated with the detection of mass 70 fragments (Cl_2^+) in the positive ion detector. The reaction channels that contribute to this cross section are also shown.

DISCUSSION

In general, the shapes of the measured cross sections for $e^- + \text{Cl}_2^-$ collisions are similar to those obtained by Pedersen *et al.* [21] in their study of $e^- + \text{F}_2^-$ collisions. There is however one interesting exception. In the present work we observe a broad peak just above threshold in the cross section for the reactions that produce one neutral mass 35 particle (see upper part of Fig. 5). The maximum of the peak is ~ 15 eV above the threshold of the cross section and importantly the structure was not present in the corresponding cross section for the $e^- + \text{F}_2^-$ system. The structure does not appear in the cross section for the $\text{Cl}^+ + \text{Cl} + 3e^-$ channel that was measured using the positive ion detector. This is to be expected since the threshold for the reaction is higher than the energy of the peak maximum. In fact, as can be seen in Fig. 5, the $\text{Cl}^+ + \text{Cl} + 3e^-$ channel, which has a threshold of 17.8 eV, makes a contribution that coincides with the high energy side of the peak and only serves to detract from its sharpness. Our measurements clearly demonstrate that the peak is associated with the $\text{Cl}^- + \text{Cl} + e^-$ dissociation channel. It was not, however, possible to directly study this channel. We were unable to detect Cl^- ions with the present arrangement since their trajectory was close to the trajectory of the Cl_2^- ion beam (see Fig. 2). The lower part of Fig. 5 indicates that the peak structure disappears when a grid is placed in front of the neutral particles detector. This in fact is not what is happening. The falling high energy side of the peak coincides with the increasing cross section for the $\text{Cl} + \text{Cl} + 2e^-$ reaction, which has a threshold of 4.8 eV, the contribution from this channel distorts the shape of the peak in the composite cross section by making it appear flatter.

What is the origin of this peak? We can eliminate electron-impact excitation from the ground state of Cl_2^- to excited bound or repulsive states since such a transition would produce a step-like structure in the cross section and not a peak. One plausible mechanism involves the transformation of kinetic energy of the incident electron into potential energy of excitation of the anion thus producing a slow electron that can be readily captured. This excitation plus capture process could produce a doubly charged negative ion in a short-lived excited state. A resonance would arise in the $\text{Cl}^- + \text{Cl} + e^-$ reaction channel if the Cl_2^{2-*} state participated in an intermediate step in the following reaction:



Dianionic resonances of this type have been observed in previous experiments involving homonuclear molecular anions such as B_2^- and C_2^- [9]. At present there are no *ab initio* calculations of the potential energy curves of electronic states of the Cl_2^{2-*} ion so we must rely at this stage on qualitative arguments. Figure 8 shows potential energy curves for Cl_2^- and Cl_2^{2-*} . These curves are not calculated. The qualitative curves in the figure are used merely to illustrate a possible mechanism for the production of an excited state of Cl_2^{2-*} with about the right amount of energy relative to the ground state of Cl_2^- . The lowest unoccupied orbital of the Cl_2 molecule is the $3p\sigma_u$, which is an antibonding orbital. The Cl_2^- ion is formed by a single occupation of

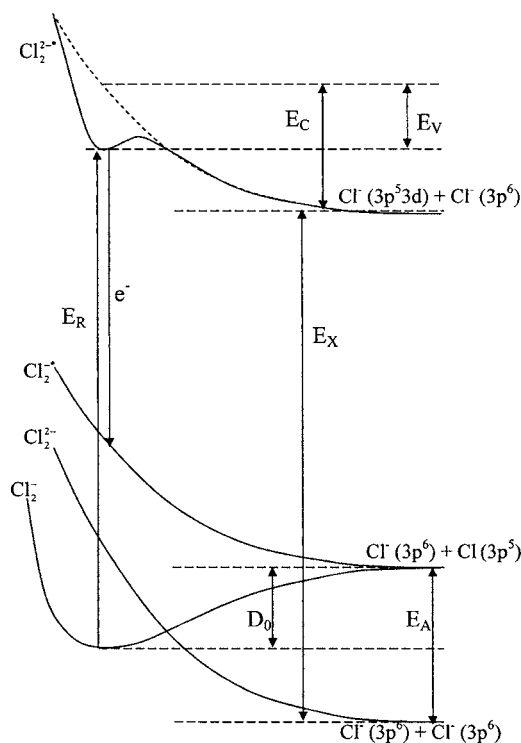


FIG. 8. A schematic energy diagram showing the relative positions of low-lying potential energy curves of the Cl_2^- ion and the proposed excited state and ground state of the Cl_2^{2-*} ion. These qualitative curves are not based on a calculation. They are shown in order to illustrate how the dianionic resonant state could be produced by an excitation plus capture mechanism and how this excited state could subsequently decay via the $\text{Cl}^- + \text{Cl} + e^-$ dissociation channel.

this orbital. If the stable, ground state Cl_2^- ion captured an additional electron it would form an Cl_2^{2-} ion in its repulsive ground state. However, if an incident electron of exactly the right energy could excite the electron from the $3p\sigma_u$ antibonding orbital to the $3d\sigma_g$ bonding orbital, while being itself captured into the $3p\sigma_u$ orbital, an Cl_2^{2-*} ion in an excited state would be formed. The bond strength of the Cl_2^{2-*} ion would then be +1, which makes it tempting to speculate that the potential curve associated with the excited state could be weakly bound. Since the $3p$ and $3d$ levels are relatively well separated in energy, the excitation energy of the dianionic state is consistent with the energy of the observed structure in the dissociation cross section. We can estimate the expected energy of the resonance by making a few assumptions. Let us assume that the excitation energy of the $3p^5 3d$ state above the $3p^6$ ground state in Cl^- is roughly the same as the energy separation of the excited $3p^4 3d$ state and the $3p^5$ ground state of Cl . There are a number of states in with configurations $3p^4 3d$ in the energy range 10.9–11.4 eV. We estimate then that the energy E_x of the excited state of Cl_2^{2-*} lies about 11 eV above its repulsive ground state. From Fig. 8 we see that the energy E_R of the excited state of Cl_2^{2-*} above the Cl_2^- ground state can be written as

$$E_R = (E_C - E_V) + (E_X - E_A) + D_0 \quad (8)$$

Approximate values of the parameters are electron affinity, $E_A = 3.61$ eV, the dissociation energy, $D_0 = 1.26$ eV, and

the excitation energy, $E_X \sim 11$ eV. The Coulomb energy, $E_C = e/4\pi\epsilon_0 R_C \sim 5.4$ eV for an internuclear equilibrium distance, $R_C = 2.65$ Å. The energy of the excited state, in eV, then becomes $E_R \sim 14 - E_V$. The internal energy E_V of the electronically excited Cl_2^{2-} could be expected to range over several eV. Thus an estimate of the resonance energy is in the range $E_R \sim 10 - 14$ eV. This range of values is in reasonable agreement with the measured energy of the center of the structure shown in the upper part of Fig. 5. The explanation of the origin of the resonance in $e^- + \text{Cl}_2^-$ collisions also explains why no resonance was observed in $e^- + \text{F}_2^-$ collisions. In this case there are no available molecular orbitals arising from atomic d orbitals since the outermost electrons reside in the $n=2$ shell.

Figure 8 also shows the most likely way that the excited state of the Cl_2^{2-} decays. Since the resonance peak modulates the cross section for the dissociation of the Cl_2^- ion via the $\text{Cl}^- + \text{Cl} + e^-$ channel, one decay mode would be to have a single electron autodetachment process that leaves the Cl_2^- ion in a repulsive state, from which it rapidly dissociates via the $\text{Cl}^- + \text{Cl}$ channel. It is also possible, but less likely, that the excited state could decay to a state of Cl_2 via two-electron autodetachment. Electrons in high lying vibrational levels of the excited state of Cl_2^{2-} , however, may preferentially decay by tunnelling through the Coulomb barrier and dissociating via the excited $\text{Cl}^- + \text{Cl}^-$ channel. The ground state $\text{Cl}^- + \text{Cl}^-$ channel would correspond to the repulsive ground state of the Cl_2^{2-} ion.

SUMMARY

We have investigated the collisional interaction between an electron and the Cl_2^- ion over an energy range 0–200 eV.

The absolute cross section measurements show that the process of dissociation dominates over that of detachment in this energy range. Detachment is suppressed, and therefore dissociation is enhanced, as a result of the fact that the ground state potential energy curves of Cl_2^- and Cl_2 have equilibrium internuclear distances that are separated by about 0.6 Å. As a consequence both direct detachment and autodetachment via low-lying repulsive curves of Cl_2^- become improbable. Dissociation via the repulsive curves becomes the most probable process. Detachment plus dissociation most likely proceeds via transitions to higher-lying repulsive curves of the Cl_2 molecule. No such states are known from theory at this time. The most significant outcome of this work is the observation of a structure in the cross section in the $\text{Cl}^- + \text{Cl} + e^-$ channel. We interpret this structure as a resonance arising from the production of the dianion Cl_2^{2-} in an excited state following an excitation plus capture process, although there is no quantitative theoretical evidence at this time. The mechanism we propose for the production of the excited state of the dianion should be applicable to other molecular and cluster negative ions. In particular, one would expect to find similar dianionic resonances in the electron impact dissociation cross sections of the negative ions of heavier halogens.

ACKNOWLEDGMENTS

This work was supported by the Swedish Research Council and the HIP program of the EC under Contract No. HPRN-CT-2000-00142. Financial support was also provided by the Northern Ireland Department of Higher and Further Education, Training and Employment.

-
- [1] G. Tisone and L. M. Branscomb, *Phys. Rev. Lett.* **17**, 236 (1966).
 - [2] D. F. Dance, M. F. A. Harrison, and R. D. Rundell, *Proc. R. Soc. London, Ser. A* **299**, 525 (1967).
 - [3] B. Peart, D. S. Walton, and K. T. Dolder, *J. Phys. B* **3**, 1346 (1970).
 - [4] B. Peart and D. S. Walton, *J. Phys. B* **4**, 88 (1971).
 - [5] P. Defrance, W. aeyns, and F. Brouillard, *J. Phys. B* **15**, 3509 (1982).
 - [6] L. H. Andersen *et al.*, *Phys. Rev. Lett.* **74**, 892 (1995).
 - [7] L. Vejby-Christensen *et al.*, *Phys. Rev. A* **53**, 2371 (1996).
 - [8] L. H. Andersen *et al.*, *Phys. Rev. A* **58**, 2819 (1998).
 - [9] H. B. Pedersen *et al.*, *Phys. Rev. A* **60**, 2882 (1999).
 - [10] A. LePadellec *et al.*, *J. Phys. B* **35**, 3669 (2002).
 - [11] K. Fritioff *et al.*, *Phys. Rev. A* **68**, 012712 (2003).
 - [12] K. Fritioff *et al.*, *Phys. Rev. A* **69**, 042707 (2004).
 - [13] M. K. Scheller, R. N. Compton, and L. S. Cederbaum, *Science* **270**, 1160 (1995).
 - [14] L. H. Andersen *et al.*, *J. Phys. B* **29**, L643 (1996).
 - [15] H. B. Pedersen *et al.*, *Phys. Rev. Lett.* **81**, 5302 (1998).
 - [16] A. LePadellec *et al.*, *J. Chem. Phys.* **115**, 10671 (2001).
 - [17] K. Fritioff *et al.*, *J. Phys. B* **37**, 2241 (2004).
 - [18] S. N. Schauer, P. Williams, and R. N. Compton, *Phys. Rev. Lett.* **65**, 625 (1990).
 - [19] L. G. Christophorou and J. K. Olthoff, *J. Phys. Chem. Ref. Data* **28**, 131 (1999).
 - [20] A. Neau *et al.*, *J. Chem. Phys.* **113**, 1762 (2000).
 - [21] H. B. Pedersen *et al.*, *Phys. Rev. A* **63**, 032718 (2001).
 - [22] T. Leininger and F. X. Gadea, *J. Phys. B* **33**, 735 (2000).
 - [23] M. Larsson and R. Thomas, *Phys. Chem. Chem. Phys.* **3**, 4471 (2001).